PCCP

Accepted Manuscript

ROYAL SOCIETY OF CHEMISTRY

www.rsc.org/pccp

Journal Name

ARTICLE TYPE

Cite this: DOI: 10.1039/xxxxxxxxxx

Dioxygen activation in Cu-amyloid β complex †

Andrea Mirats,[a] Jorge Alí-Torres,[b] Luis Rodríguez-Santiago,[a] Mariona Sodupe[a] and Giovanni La Penna,*[c‡]

Received Date
Accepted Date

DOI: 10.1039/xxxxxxxxxx

www.rsc.org/journalname

We investigate, by means of density-functional theory, the binding of dioxygen to Cu(I)-amyloid β (Aβ), one of the first steps in the oxidation of ascorbate by dioxygen. Cu, Aβ, ascorbate and dioxygen are all present in the synapse during neurodegeneration, when the species above can trigger an irreversible oxidative stress inducing the eventual death of neurons. The binding of dioxygen to Cu(I) is possible and the role in dioxygen activation of Cu ligands and of residues in the first coordination sphere is described in atomic detail. Dioxygen is activated when a micro-environment suitable for a square-planar Cu^{2+} coordination is present and a negatively charged group like Asp 1 carboxylate takes part in the Cu coordination *anti* to O_2.

Introduction

During the on-set of Alzheimer's disease copper ions, ascorbate, dioxygen and pathologically accumulated amyloid β (Aβ) peptides are all present in the synaptic region of neurons[1,2]. Since Cu complexes catalyze the formation of reactive oxygen species (ROS) and Cu forms a stable complex with Aβ, the anomalous production of ROS by Cu-Aβ can trigger the neurodegeneration towards an irreversible oxidative pathway. Particularly important in this context is the amyloid polymorphism, that allows the formation of oligomeric complexes[3,4] with peculiar reactivity and catalytic properties. For instance, *in vitro* studies of Cu-Aβ show that Aβ monomers and fibrils are less efficient in producing hydrogen peroxide than oligomers[5]. Also, Aβ oligomers are more neurotoxic than monomers[6,7]. Amyloid polymorphism can explain the difficulties in reproducing ROS activity of Cu-Aβ complexes even *in vitro*[8]. The role of Cu-Aβ as catalyst in the ROS production is, therefore, still elusive.

According to the initial proposal by A. Rauk and coworkers[9], we exploit the mechanism for the oxidation catalysis displayed in Fig. 1. DH_2 is the reduced form of ascorbic acid and $DH^{\cdot}$ is its one-electron oxidized form (ascorbyl radical). Steps 1 and 3 are

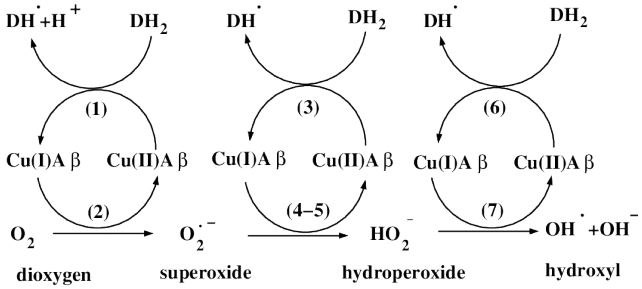

Fig. 1 Summary of proposed one-electron transfers involved in the oxidation of ascorbate by dioxygen catalyzed by Cu complexes.

the one-electron transfer steps involving the reductant DH_2. After the initiation (step 1) involving the production of a small amount of Cu^+, the activation of dioxygen to a Cu-bound superoxide (step 2) is proposed. Activation of dioxygen to superoxide may occur because of the presence of suitable coordinations for Cu^{2+} to Aβ, in square-planar coordinations involving an end-on Cu-bound O_2, while steps 3-4 identify a globally down-hill proton-coupled electron transfer[9,10]. The oxidation is then propagated by hydrogen peroxide that is released by the complex (step 5). This latter can eventually be splitted into hydroxyl radical by other Cu^+ complexes in the environment[11] (steps 6-7).

There is a debate about the life-time of initially Cu-bound superoxide and the accessibility to superoxide of other reactant molecules in the synaptic region. This issue is important in order to understand if superoxide scavenging reactions can hinder

[a] *Departament de Química, Universitat Autònoma de Barcelona, 08193 Bellaterra, Barcelona, Spain; Fax: +34935812920; Tel: +34935813031; E-mail: Mariona.Sodupe@uab.cat*
[b] *Departamento de Química, Universidad Nacional de Colombia - Sede Bogotá, 111321 Bogotá, Colombia*
[c] *Institute for chemistry of organo–metallic compounds (ICCOM), National Research Council of Italy (CNR), via Madonna del Piano 10, I-50019 Sesto Fiorentino, Firenze, Italy; Fax: +390555225203; Tel: +390555225264; E-mail: glapenna@iccom.cnr.it*
† Electronic Supplementary Information (ESI) available: [details of any supplementary information available should be included here]. See DOI: 10.1039/b000000x/
‡ Associated to the National Institute for Nuclear Physics of Italy (INFN, section Roma-Tor Vergata).

the ascorbate oxidative pathway, when the cells are not able to take under control the produced hydrogen peroxide. The identification of superoxide as an intermediate has been always difficult also *in vitro* [12]. Computational models are particularly useful to elucidate mechanisms involving labile intermediates. On the other hand, computational results strongly depend on the chosen model: chemical groups in the second Cu-coordination sphere influence the reactivity of Cu; geometrical constraints acting on the ligand proteins change the orientation of ligand atoms; the accessibility to the water solvent modulates the possible replacement of protein ligand atoms with water.

The binding of Cu in reduced (Cu(I)) and oxidized (Cu(II)) forms to Aβ has been extensively investigated with *in vitro* studies [2,13]. Most of these data have been interpreted with structural models based on electronic structure calculations [14–16], also with the aim of estimating the reorganization of the peptide ligand with the change of oxidation state [11,17].

On the basis of this knowledge about Cu-Aβ interactions, this work extends the range of hypothetical A$\beta-$Cu$-O_2$ coordinations proposed by A. Rauk and coworkers [9,10], and shows that the stability and nature of the ternary complex depend on the way Cu is bound to Aβ. The structural disorder (polymorphism) of the Aβ peptide together with its affinity for Cu in both oxidation forms, suggests a peculiar role of the Aβ ligand in the local (*in situ*) activation of dioxygen, once triplet dioxygen reach the Cu(I) coordination site. This latter is the relevant initial oxidation state of Cu in dioxygen activation, while the extent of final Cu oxidation depends on the chance for an efficient electron transfer to the bound dioxygen.

Methods

We performed electronic structure calculations, within standard density-functional theory (DFT) approximations, for several possible Aβ-Cu-O_2 configurations obtained by different approaches. We used the hybrid M06-2X exchange functional [18] because results obtained with a range of different functionals and perturbation methods indicate that M06-2X provides a reasonably good description of both the second ionization energy (IE) of Cu and the electron affinity (EA) of dioxygen (ESI†, Table S1), which is essential for a proper description of the charge transfer Cu(II)$\cdots O_2^{\cdot -}$ species.

Our converged DFT set-up includes a localized basis-set of type 6-31+G(d) for N, O, C and H atoms, and LANL2DZ for Cu, the atomic core of this latter described with a pseudo-potential. This basis-set has been shown to be a cost effective basis, structural parameters being only slightly modyfied when further enlarging the basis-set (ESI†, Table S2). We modelled solvent effects with an implicit polarizable continuum model (SMD) [19] in all geometry optimizations, performed with the Gaussian09 code [20] (see ESI† for details).

The model construction was performed via two different approaches. In one approach (models **Ia**, **IIa** and **IIc**) the complex was built by adding dioxygen to truncated models of the Cu(I)-Aβ(1-16) structures previously obtained in Ref. 17 after reduction of monomeric Cu(II)-Aβ(1-16) (see ESI† for details). These models enclose the experimentally proposed coordination spheres, on the basis of electron paramagnetic resonance (EPR) spectroscopic measurements. The models were built combining homology modelling and quantum chemical calculations, and represent, respectively, the so-called component I (**Ia**) at lower pH [21,22] and component II (**IIa** [13] and **IIc** [23]) at higher pH. In a second approach (models **1**-**15**) the initial structures were built following the identification of Cu-bound states for hydroperoxide in Cu(I)-Aβ(1-16) complexes [11]. In the latter case, we converted hydroperoxide into dioxygen, keeping the bath of 311 water molecules. This combination of approaches allows the exploitation of 14 A$\beta-$Cu(I)$-O_2$ relaxed configurations. The initial configurations used in the second approach included information concerning Aβ dimers. In fact, the Aβ peptide was represented by the two peptides **DGGGGHD**-$NHCH_3$ and CH_3CO-**HH**-$NHCH_3$, representing, respectively, sequence **DAEFRHD** in Aβ(1-7) and sequence **HH** in Aβ(13-14). In some of these configurations (**9**-**15**) the second peptide (Aβ(13-14)) was extracted from a second Aβ(1-16) peptide, thus allowing the representation of dimeric Aβ(1-16)-Cu-Aβ(1-16) in terms of Aβ(1-7)-Cu-Aβ(13-14) simplified models.

To compute energies and to characterize the models, these latter were simplified to the first Cu-coordination sphere, including, in 11 cases, water molecules in the Cu-second coordination sphere selected from the thermal bath when within 2 Å from the added dioxygen molecule. Geometry optimizations were performed for these simplified models (see ESI† for details).

Results

In the computational experiments reported in Refs. 11 and 17, we showed that the ability to oxidize Cu(I) in Aβ strongly depends on the availability of ligands that stabilize a suitable environment for Cu(II), *i.e.* where valence 4-5 is accessible to Cu. When the Cu(I)-Aβ configuration does not allow the income of 4-5 ligands (including water or reactant peroxide molecules), the reduction potential is high and Cu(II) behaves as an oxidant. This occurs because the reduced form of Cu-Aβ does not change significantly its energy by changing the number of ligands in the first Cu-coordination sphere, while the oxidized form has a high energy when the number of ligands is smaller than 3.

The formation energy of each Cu$-$A$\beta-O_2$ ternary complex (E_f) is defined as the energy difference for the sequential addition of ligands to a seed Cu(I)$-$Im aquo complex, *i.e.* the reaction:

$$(\mathrm{metIm}_{\delta/\varepsilon})\mathrm{Cu(I)}\text{-}(\mathrm{H_2O})_3 + \mathrm{L} + \mathrm{O_2} \longrightarrow (\mathrm{metIm}_{\delta/\varepsilon})\mathrm{LCu(I)}\text{-}\mathrm{O_2} + 3\,\mathrm{H_2O} \quad (1)$$

where L indicate all the ligands additional to the 4-methylimidazole (protonated in position Nδ or Nε, metIm_δ or $\mathrm{metIm}_\varepsilon$, respectively) in each of the Cu-Aβ truncated models analysed (see ESI†). In order to measure the energy change in step 2 of Fig. 1 (E_2), in each of the 14 minimal energy configurations that have been modelled as product, the following procedure is performed. First, the geometry of the complex is optimized with O_2 at binding distance from Cu. Then the dioxygen molecule is manually moved apart from Cu and the close-by energy minimum is then computed by optimizing the geometry of the Cu-unbound dioxygen complex. This manipulation allows an estimate of the energy

cost for superoxide formation in the O_2 Cu-bound state (product in step 2) with respect to the O_2 unbound state (reactant in step 2). The comparison among the energy differences E_2 for the 14 configurations and the characterization of the electronic structure of the two states, allow the identification of the interactions favouring or disfavouring the Cu-bound activated superoxide form of the ternary complex. The results are summarized in Table 1 and some representative structures are displayed in Fig. 2.

Table 1 Formation energy of each model (E_f, Eq. 1), energy difference between Cu-bound and unbound states (E_2, *i.e.* energy difference in step 2 of Fig. 1) and the list of Cu ligands complementing O_2 binding. Im is the imidazole group of the His sidechain. For configuration **11** the bound state is not an energy minimum. Energies are in kcal/mol.

model	group	E_f	E_2	Cu coordination
Models derived from Aβ monomers				
Ia	C	-16.3	0.4	2Im+N/O(Asp 1)
IIa	A	-19.7	-1.4	3Im
IIc	-	-15.2	-3.6	Im+N(Asp 1)+N(Ala$^-$ 2)
1	A	-28.5	4.5	3Im
2	B	-29.6	1.7	2Im+H_2O
5	B	-33.1	7.3	2Im+H_2O
7	B	-33.1	13.8	2Im+H_2O
8	C	-25.3	1.0	2Im+N(Asp 1)
Models derived from Aβ dimers				
9	C	-37.4	2.3	2Im+N(Asp 1)
10	D	-35.5	5.1	Im+N(Asp 1)
11	B	-36.0	-	2Im
13	A	-24.1	3.0	3Im
14	D	-33.3	-0.7	Im+N/Oδ(Asp 1)
15	A	-25.4	-0.6	3Im

The reasons of the differences in binding energy and, therefore, in the spin configuration for the Cu-bound state can be understood if the 14 models are divided in four groups, according to the respective coordination topology and ranked in order of the decreasing number of His sidechains binding Cu, *i.e.* in order of decreasing His crowding.

Models **1**, **13**, **15** and **IIa** belong to the group of configurations where Cu is bound to 3 imidazole rings of three different His sidechains (group **A**, hereafter). The fourth Cu valence is filled by O_2 in the end-on coordination. Only in model **13** the carbonyl oxygen of Asp 1 is at 2.3 Å from Cu *anti* to O_2, thus forming an asymmetric 5-coordinating Cu complex. In models **1** and **13** the Cu-bound state is at a slightly higher energy compared to the unbound Cu(I) state, because of the Cu-coordination distortions that prevent the formation of a stable square-planar coordination for Cu^{2+} (ESI†, Figs. S2-S3). Model **15** shows that a stable square-planar coordination for Cu can be easily achieved if one of the three His sidechains belongs to a different peptide (ESI†, Fig. S3 and Fig. 2). In this form, the spin density on Cu is 0.73 electrons, *i.e.* larger than 0.66 that is achieved for the model **IIc** with lowest E_2 and where larger spin delocalization is observed. The low stability of Cu(I) surrounded by more than 2 His sidechains in a pseudo square-planar Cu coordination has been already reported[14] and explained with the large chance to adapt the coordination to the stable digonal His-Cu(I)-His coordination.

Models **2**, **5** and **7** display two imidazole rings of His and one water molecule bound to Cu (group **B**, hereafter), with O_2 attempting to fill the fourth Cu valence. Model **11** lacks also of the third ligand, the water molecule, thus forming a digonal configuration. These four configurations resemble, in terms of the non-O_2 ligands, those observed for the monomeric Cu(I)-Aβ complex[14]. In all cases the O_2 Cu-unbound state is more stable than the Cu-bound state and the N-Cu-N angle, that in some cases is smaller than 180° (**2** and **7**), can be easily relaxed to 180° via a His sidechain rearrangement. This event is displayed by model **11**, where a large structural distortion upon the O_2 unbinding (ESI†, Fig. S3) produces a stable Im-Cu(I)-Im digonal coordination. This latter model prevents the binding of O_2 to Cu, consistently with the measured sluggish reactivity of Cu(I)-Aβ when this latter forms a stable digonal Cu(I) coordination[14].

Models **Ia**, **8** and **9** display two imidazole rings of His bound to Cu together with N(Asp 1) and O_2 (group **C**, hereafter). Again, in all of these cases the release of dioxygen is exothermic.

Models **10** and **14** display one single imidazole ring bound to Cu, together with N(Asp 1) and O(Asp 1) or Oδ(Asp 1), respectively, complementing the binding to O_2 (group **D**, hereafter). The O_2 is *anti* to the carboxylate group only in model **14** and the spin density on Cu is 0.70. E_2 for **14** indicates that superoxide formation is exothermic, with a value lower than the ideal case of **IIa** belonging to group **A**.

According to E_2 values, the larger exothermicity is observed for **IIc**, due to the fact that Cu^{2+} is stabilized by the presence of a negatively charged ligand in the coordination sphere with a square-planar geometry. It must be noticed that the high stability of Cu^{2+}-Aβ at high pH (model **IIc**) is responsible of the low reduction potential of Cu-Aβ at high pH[17,24]. Therefore, for model **IIc** step 1 is hindered and the whole mechanism is not active. In this configuration the spin density on Cu in the O_2-bound state is 0.66.

The favourable energy change of O_2 binding in the superoxide form displayed by model **14** is caused by two effects due to the *anti* coordination of the carboxylate with respect to the end-on O_2 ligand. One is the stability of the Cu^{2+} square-planar complex in the product (see structure of model **14** in ESI†, Fig. S3); the second effect is the instability of the perturbed digonal Cu^+ configuration that is formed upon O_2 release. The latter perturbation is due to the repulsion for hard ligands approaching Cu^+ from a direction that is orthogonal to the axis formed by two other soft ligands (N imidazole or amino atoms) binding Cu. This latter repulsion has been reported in many investigations of the Cu(I)-Aβ complex[14,17].

In all the **1**-**15** models, one or two water molecules interact with the Cu-bound O_2 molecule via hydrogen-bonds. We remind that the initial structures for these 11 models were selected as those with Cu accessible to water among the 16 Cu-Aβ(1-16) models simulated via first-principle molecular dynamics at the temperature of 300 K and in the presence of 311 water molecules mimicking the thermal bath[11]. The energy contribution of $O_2\cdots H_2O$ interactions is, however, rather constant among the investigated models, while the contribution of the Asp 1 carboxylate is more sporadic.

The formation energy of the different configuration changes more because of mechanical distortions of ligands than because of

the change in the type of coordination. For instance model **8** has a larger formation energy than **9** because of the constraints induced by the monomeric peptide in the former compared to the latter that is obtained by a dimer. On average, the monomeric forms (excluding **IIc**) have a formation energy of -27±6 kcal/mol, compared to -32±5 of dimeric forms. The larger formation energy of monomers compared to dimers is due to the ligand distortions required to wrap regions 1-7 and 13-14 of the same Aβ(1-16) peptide around the same Cu ion in monomeric forms.

A direct interaction between Cu and Asp 1 carboxylate has been detected in a few experiments concerning Cu-Aβ[25,26]. The conditions for this direct interactions are likely not well reproducible, because the statistical weight of such interaction depends on many factors. Here we remark that model **14** was built starting with a Cu ion interacting with two Aβ(1-16) peptides, conversely to models **1**-**8**, built on the basis of monomers. The Asp 1 residue in model **14** and the His 6 residue in model **15** belong to one monomer, while the partner His sidechains (one in **14**, two in **15**) belong to the other monomer in the initial model (Fig. 2). This condition mimics the transient interaction between an Aβ peptide weakly bound to Cu via one or two His sidechains and a second Aβ segment offering the N-terminus to this partially formed binding site. Previous models of a hypothetical quaternary complex between Aβ−Cu−O_2 and a deprotonated ascorbyl radical[27] also displayed an efficient O_2 activation to superoxide due to the negatively charged ascorbyl ligand *anti* to Cu−O_2 binding.

Interestingly, the models that display the larger propensity for O_2 activation here addressed are different from those activating hydroperoxide in step 7 of Fig. 1. According to previous calculations[11] HO_2^- activation occurs in configurations similar to groups **B** and **C** here described. This observation suggests a significant reorganization of Cu coordination sphere in steps 3-5 and an alternative release of H_2O_2 once this reorganization be hindered by the peptide mechanics.

Conclusion

Dioxygen activation to superoxide by Cu-Aβ complexes is a crucial step in the the generation of ROS species, triggering initial molecular events, hallmark of Alzheimer's disease, to an irreversible oxidative stress. The present study reports computational models of the O_2 binding to Cu-Aβ for a range of hypothethical configurations, defined on the basis of experimental data. In all cases, spin density values for the bound Aβ-Cu-O_2 complexes indicate a significant Cu^{2+} character and, consequently, a strong charge transfer to superoxide. Results also show that superoxide formation is more favourable in His rich distorted Cu coordinations or when there is a negatively charged ligand such as Asp 1 carboxylate *anti* to O_2. Overall, the environments displayed by models **IIa**, **14** and **15** appear to be accessible transient states connecting the structures revealed by experiments.

The reported calculations do not provide information about eventual superoxide dismutase (SOD) activity of the Cu-Aβ complex, because the approach of $O_2^{\cdot -}$ to Cu(II)-Aβ has not been investigated. Nevertheless, the Cu-Aβ species here addressed may compete with other oligomeric species that can be good catalysts for superoxide dismutation. Indeed, structures that are good candidates for these latter species have been observed for Zn-Aβ(1-16) oligomers[29].

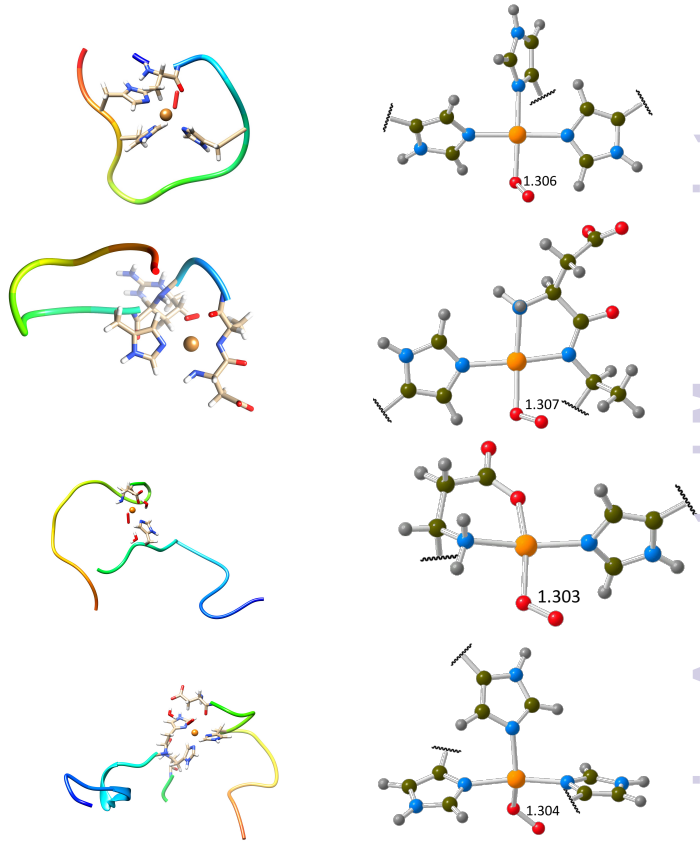

Fig. 2 Structures of models **IIa**, **IIc**, **14** and **15** (from top to bottom) with the reconstructed 1-16 segments displayed as tubes interpolating the backbone atoms. C is yellow (grey in the right panels), N is blue, O is red, Cu is orange. Atomic and bond radii are arbitrary. Only atoms belonging to Cu-binding sidechains are displayed. The Chimera[28] program is used for molecular drawings.

Acknowledgments

We thank Peter Faller (LCC-CNRS, Toulouse) for the stimulating discussions. GLP thanks PRACE (Partnership for advanced computing in Europe) and CALMIP (Toulouse, F) for computational resources (projects 063 and 1039, respectively). This work has been concluded within the COST action CM1305 (ECOSTBio). Financial support from MINECO and the Generalitat de Catalunya, through CTQ2014-59544-P and 2014SGR-482 projects, respectively, and access to supercomputing facilities (QCM-2014-1-0019) is gratefully acknowldeged.

References

1 *Metal Ions in Neurological Systems*, ed. W. Linert and H. Kozlowski, Springer, 2012.
2 P. Faller and C. Hureau, *Coord. Chem. Rev.*, 2012, **256**, 2127–2128.
3 Y. Miller, B. Ma and R. Nussinov, *Coord. Chem. Rev.*, 2012, **256**, 2245–2252.
4 T. M. Ryan, N. Kirby, H. D. T. Mertens, B. Roberts, K. J. Barnham, R. Cappai, C. L. L. Pham, C. L. Masters and C. C. Curtain, *Metallomics*, 2015, **7**, 536–543.
5 R. C. Nadal, S. E. J. Rigby and J. H. Viles, *Biochemistry*, 2008, **47**, 11653–11664.
6 M. Rózga and W. Bal, *Chem. Res. Toxicol.*, 2010, **23**, 298–308.
7 J. E. Straub and D. Thirumalai, *Annu. Rev. Phys. Chem.*, 2011, **62**, 437–463.
8 D. Ciregna, E. Monzani, G. Thiabaud, S. Pizzocaro and L. Casella, *Chem. Commun.*, 2013, **49**, 4027–4029.

9 N. Hewitt and A. Rauk, *J. Phys. Chem. B*, 2009, **113**, 1202–1209.
10 A. Rauk, *Chem. Soc. Rev.*, 2009, **38**, 2698–2715.
11 G. La Penna, C. Hureau, O. Andreussi and P. Faller, *J. Phys. Chem. B*, 2013, **117**, 16455–16467.
12 S. Parthasarathy, B. Yoo, D. McElheny, W. Tay and Y. Ishii, *J. Biol. Chem.*, 2014, **289**, 9998–10010.
13 S. C. Drew and K. J. Barnham, *Acc. Chem. Res.*, 2011, **44**, 1146–1155.
14 S. Furlan, C. Hureau, P. Faller and G. La Penna, *J. Phys. Chem. B*, 2010, **114**, 15119–15133.
15 J. Alí-Torres, J.-D. Maréchal, L. Rodríguez-Santiago and M. Sodupe, *J. Am. Chem. Soc.*, 2011, **133**, 15008–15014.
16 S. Furlan and G. La Penna, *Coord. Chem. Rev.*, 2012, **256**, 2234–2244.
17 J. Alí-Torres, A. Mirats, J.-D. Maréchal, L. Rodríguez-Santiago and M. Sodupe, *J. Phys. Chem. B*, 2014, **118**, 4840–4850.
18 Y. Zhao and D. G. Truhlar, *Theor. Chem. Acc.*, 2008, **120**, 215–241.
19 A. V. Marenich, C. J. Cramer and D. G. Truhlar, *J. Phys. Chem. B*, 2009, **113**, 6378–6396.
20 M. J. Frisch, *et al.*, *Gaussian 09, Revision C.01*, Gaussian Inc., Wallingford CT, USA, 2010.
21 S. C. Drew, C. L. Masters and K. J. Barnham, *J. Am. Chem. Soc.*, 2009, **131**, 8760–8761.
22 P. Dorlet, S. Gambarelli, P. Faller and C. Hureau, *Angew. Chem. Int. Ed.*, 2009, **48**, 9273–9276.
23 C. Hureau, Y. Coppel, P. Dorlet, P. L. Solari, S. Sayen, E. Guillon, L. Sabater and P. Faller, *Angew. Chem. Int. Ed.*, 2009, **48**, 9522–9525.
24 C. Hureau and P. Dorlet, *Coord. Chem. Rev.*, 2012, **256**, 2175–2187.
25 Y. El Khoury, P. Dorlet, P. Faller and P. Hellwig, *J. Phys. Chem. B*, 2011, **115**, 14812–14821.
26 C. Z. Gomez-Castro, A. Vela, L. Quintanar, R. Grande-Aztatzi, T. Mineva and A. Goursot, *J. Phys. Chem. B*, 2014, **118**, 10052–10064.
27 K. J. Barnham, F. Haeffner, G. D. Ciccotosto, C. C. Curtain, D. Tew, C. Mavros, K. Beyreuther, D. Carrington, C. L. Masters, R. A. Cherny, R. Cappai and A. I. Bush, *FASEB J.*, 2004.
28 E. F. Pettersen, T. D. Goddard, C. C. Huang, G. S. Couch, D. M. Greenblatt, E. C. Meng and F. T. E., *J. Comput. Chem.*, 2004, **25**, 1605–12.
29 P. Giannozzi, K. Jansen, G. La Penna, V. Minicozzi, S. Morante, G. C. Rossi and S. Francesco, *Metallomics*, 2012, **4**, 156–165.